R. & M. No. 2735
(11,837)
A.R.C. Technical Report

MINISTRY OF SUPPLY

AERONAUTICAL RESEARCH COUNCIL
REPORTS AND MEMORANDA

Flow Through a Helicopter Rotor in Vertical Descent

By
P. BROTHERHOOD, D.L.C.

LONDON: HER MAJESTY'S STATIONERY OFFICE
1952
FOUR SHILLINGS NET

Flow Through a Helicopter Rotor in Vertical Descent

By

P. BROTHERHOOD, D.L.C.

COMMUNICATED BY THE PRINCIPAL DIRECTOR OF SCIENTIFIC RESEARCH (AIR), MINISTRY OF SUPPLY

*Reports and Memoranda No. 2735**
July, 1949

Summary.—Flight tests have been made on a *Hoverfly I* helicopter to investigate the types of flow associated with various rates of vertical descent. At the same time measurements of the performance were made.

The results are analysed by two different methods to produce characteristic curves for the rotor and are compared with data obtained from wind tunnel tests on model propellers at negative rates of advance.

The information was obtained from the *Hoverfly I* helicopter but it is thought that the results can be applied to any other helicopter of similar size.

1. *Introduction.*—The performance of a helicopter in vertical flight cannot be predicted by normal propeller theory over a range of vertical descent. Propeller theory is based on the formation of an ideal wake extending to infinity in a direction parallel to the thrust.

Hovering flight represents the limiting case for these conditions. When the power supplied to the rotor is reduced from that required for hovering, the helicopter begins to descend, and air is directed against the bottom of the rotor disc. The development of an ideal wake is then impeded, and the rotor is surrounded by a vortex of turbulent air. This working condition is termed the vortex ring state and little is known of its physical construction.

When the power supplied to the rotor becomes less than that required to overcome the profile drag of the blades, the rotor passes into the windmill brake state of operation, a particular case of which is autorotation. The flow is turbulent in the initial part of the windmill brake state of operation, and the condition of flight at which an ideal wake is re-established is practically outside the range of flight of the helicopter. Thus the vortex theory is inapplicable to the helicopter over most of the vertical descent range.

Wind-tunnel tests had been made in the past (R. & M. 1014[1]) on propellers of fine pitch at negative rates of advance, enabling an empirical relationship to be found between the axial and induced velocities. The so-called characteristic curve of a propeller was then completed, from which thrust coefficients for any working condition could be deduced.

A brief check on the validity of applying this characteristic curve to a helicopter rotor was made during the general handling tests on the *Hoverfly I*, and the results published in Ref. 2. The general agreement, although there were several serious discrepancies, warranted a thorough investigation with improved experimental technique.

* R.A.E. Report Aero. 2272, received 15th October, 1948.

This report deals with flight tests made on the *Hoverfly* to determine the performance in vertical descent, and gives a presentation of the results in new alternative forms suggested by Lock (R. & M. 2673[6]) and Hafner[3]. These allow a more ready interpretation of the conditions of flow in the various working states of the propeller or helicopter rotor.

An investigation of the various types of flow in vertical descent using smoke filaments has also been made.

2. *Description of Aircraft.*—The *Hoverfly I*, used in these tests was a standard *Sikorsky R-4B* aircraft. It has one main three-bladed rotor, and a vertical tail rotor. Power is derived from a Warner 180 h.p. air-cooled radial engine. The maximum permissible all-up weight is 2800 lb.

The aerofoil section at the root of the blades is NACA 0012·5, and at the tip 0012. The inboard part of the blade is of constant chord, followed by a straight taper to a rounded tip. The blade is untwisted.

More complete descriptions of the *Hoverfly I* and of the blades are given in R. & M's. 2431 and 2521[4,5] respectively.

3. *Instrumentation.*—3.1. *The Smoke Installation.*—A steel tube, 2·5 in. internal diameter, was fixed at the top of the port undercarriage leg. It was braced in a position at right-angles to the main rotor shaft by four wires attached to the fuselage. The tube projected two feet beyond the edge of the rotor disc. In the initial tests, a smoke generator was fixed to the boom at 0·7 of the rotor radius, giving a single smoke filament issuing from this point. For the rest of the tests an improved method with four smoke filaments was used. The smoke generator was carried at the extremity of the tube and the smoke conducted along the tube to four exit holes in the upper surface, situated at positions 0·42, 0·63, 0·85 and 1·05 of the rotor radius. The smoke exit holes, nominally $\frac{1}{2}$ in. in diameter, were slightly increased in size progressively towards the rotor shaft in order to ensure an equal quantity of smoke passing through each hole.

The type of smoke generator used was a Wessex daylight distress signal Type S, in which potassium chlorate oxidises a fuel impregnated with an orange dye which is volatilised by the heat of combustion. The smoke generator was fired electrically from the cockpit, and emitted a deep orange smoke for a duration of about thirty seconds.

A 35 mm ciné camera was fitted on the rear fuselage of the helicopter photographing forward and to port in order to record the smoke patterns.

A diagrammatic sketch of the layout is given in Fig. 1.

3.2. *Measurement of Rate of Descent, Pitch and Engine Conditions.*—The rate of descent, main rotor pitch and engine conditions were recorded simultaneously in an automatic observer, the camera speed being twenty-four frames per second.

The rate of descent was determined from an altimeter and clock, but a rate of climb indicator was also fitted to provide a rough check. The static pressure for both altimeter and rate of climb indicator was obtained from a trailing static suspended 60 ft below the aircraft.

The trailing static was specially designed for vertical flight work, and consisted of a brass tube extension (1 ft in length and 0·5 in. in diameter) to the rubber suspension tubing. It had static holes in the wall of the tube at a position two inches from the lower end, which was sealed.

The indication of the pitch angle was Desynn transmitted from the main pitch change rod, and the absolute value determined from a ground calibration.

The engine power was obtained from the measurements of manifold pressure and r.p.m.

3.3. *The Correlation of the Two Camera Films.*—The synchronisation of the automatic observer record and the camera photographing the smoke streamers was achieved by arranging for a small electric bulb in the automatic observer to be flashed when a picture of the smoke was taken by the tail camera.

4. *Flight Technique.*—The tests were started at a height of 3,500 ft. The required rotor speed and engine manifold pressure were selected by the pilot at normal forward speed. The speed was then reduced towards zero and the pilot then guided the helicopter according to the instructions of the observer who was noting the behaviour of the suspended static trailing below the aircraft. Any relative horizontal motion was immediately apparent by bowing of the rubber suspension tube.

When the helicopter was descending vertically, the smoke generator was fired and both the tail camera and automatic observer camera were operated simultaneously in two second bursts every five seconds during the descent. Despite continuous corrections by the pilot, it was found extremely difficult to maintain true vertical descent for any length of time, particularly when the rate of descent was between 900 and 1900 ft/min.

Within this range stick vibration and ' shuddering ' of the whole aircraft were very pronounced, and the probability of the helicopter developing horizontal velocity much increased.

Great care was necessary on the part of the pilot to avoid sudden stick movements when descending vertically. These resulted in loss of control (previously mentioned in R. & M. 2431[4]) in which the helicopter pitched nose down, and a fully backward displacement of the stick was not sufficient to prevent the aircraft going into a dive. Recovery from this was normal, but the manoeuvre required a certain amount of height in which to recover, resulting in an unsatisfactory test.

Over thirty successful vertical descents were made at a main rotor speed of 225 r.p.m. over a complete range of engine powers from maximum available down to autorotation.

5. *Experimental Results.*—Agreement between the rate of descent obtained from altimeter and stopwatch, and the rate of climb indicator was good although there was sometimes a slight difference in phase when the rate of descent was changing rapidly. The rate of descent as found from the altimeter and stopwatch is the more accurate, and the rate of climb indicator was used for checking purposes only.

A typical time history of a vertical descent is shown in Fig. 2, and it will be seen that there is considerable variation in the rate of descent. It had been apparent during the tests that any small horizontal velocities greatly affected the rate of descent in the sense that it was generally decreased by such velocities.

This is shown clearly in the photographs of the smoke filaments in Fig. 2. In the left-hand picture the helicopter has developed side-slip to the right, and the rate of descent corresponding to this condition is 450 ft/min. The right-hand picture depicts conditions of flow at the same pitch angle and power, but in true vertical descent with a well-established ' vortex ring.' The rate of descent corresponding to this condition is 1,500 ft/min. It has been mentioned previously that it was impossible to maintain true vertical descent for any length of time, and this accounts for most of the variation in the rate of descent.

Another contributary cause is the mechanics of the establishment of the vortex ring itself. In the flight tests the helicopter was brought into the vortex ring state at the appropriate pitch and power from a forward flight condition by reducing the translational speed to zero. When this is achieved an initial circulation of air is set up around the rotor disc, but two further developments then take place. The circulating air as it repasses through the rotor has its velocity further increased and at the same time the vortex circulation extends its influence radially affecting more air. This causes the rate of descent to increase until the fully established vortex circulation is achieved. This cycle of events applies equally well after recovery from translational velocities developed during the descent.

It is convenient in deducing the characteristic curve for the helicopter rotor to obtain the rate of descent *vs.* rotor blade pitch angle relationship, which is given in Fig. 3. In obtaining this curve the maximum steady rate of descent from each flight (although this did not in all cases strictly pertain to true vertical descent) was plotted against its corresponding rotor blade pitch angle. The relationship between the two variables for true vertical descent conditions was then taken to be the envelope of these points with due regard to their experimental error.

Since the helicopter at its weight during the tests (2750 lb) was incapable of hovering in free air, the blade angle required for this condition of flight was obtained by correcting the value measured during previous tests at a lighter weight (R. & M. 2521[5]). The corrected blade angle was 10·8 deg, and the rate of descent *vs.* rotor blade pitch angle curve was drawn through this point.

In autorotation at the smallest possible pitch angles the rotor speed increased slightly, and the measured pitch angles were corrected to 225 r.p.m., the chosen speed for the tests.

The curve showing the relationship between the rate of descent and the power supplied by the engine to the rotor is given in Fig. 4. For reasons similar to those mentioned previously,—that horizontal velocities decrease the rate of descent for a given power (or blade pitch angle,) the curve is obtained as the envelope of the experimental points.

The engine powers were taken from the maker's charts and corrected for temperature. In order to obtain the points as plotted it was necessary to subtract the transmission loss, the engine cooling power, and the tail rotor power. These were obtained from R. & M. 2521[5]. Since the tail rotor power is a function of the main rotor torque reaction, the tail rotor power was assumed to vary linearly with the engine power.

The general expression for the combined transmission loss, engine cooling power, and tail rotor power was obtained in the form

$$22 + 0{\cdot}042 \times \text{(engine b.h.p.) h.p.}$$

From R. & M. 2521[5] the power required by the rotor to hover at a weight of 2750 lb was 181·7 h.p., and the curve showing the variation of rotor power with rate of descent is drawn through this point.

6. *The Characteristic Curve of a Propeller.*—6.1. *Explanation of Variables.*—The quantities measured during the tests are: thrust (=weight of the helicopter), blade angle, engine conditions, rotor r.p.m., and rate of descent.

It is assumed for the purposes of calculation that the axial velocity through the rotor disc (and the induced velocity) are constant over the disc area. The angle of attack of a blade element is then less than the geometric blade angle by an amount which is proportional to the axial velocity through the rotor disc. From the known thrust, blade angle, and rate of descent. this axial velocity through the rotor disc can then be calculated (*see* section 6.2, equation (1)),

Let v_i be the axial induced velocity

v_a the axial velocity of the rotor (rate of descent)

$v_i + v_a = U$

T the thrust

R the rotor diameter

ρ the air density

then by momentum theory $T = 2\pi R^2 \rho (v_a + v_i) v_i$ for normal working states, or

$$\left(\frac{T}{2\rho\pi R^2}\right)^{1/2} = \left((v_a + v_i)v_i\right)^{1/2} = U_T \quad \text{say,}$$

where U_T is termed the ' thrust velocity.' It will be noted that in hovering flight $U_T = v_i = U$.

The velocities v_i, v_a and U are now expressed as fractions of the thrust velocity U_T, *viz.*, v_i/U_T, v_a/U_T, and U/U_T. Any state of operation of a propeller or helicopter rotor may be represented by the pair of values v_a/U_T and v_i/U_T or v_a/U_T and U/U_T. The representation used by Lock (R. & M. 2673[6]) is in terms of v_a/U_T and U/U_T, where $v_a/U_T = \sqrt{(1/f)}$ and $U/U_T = \sqrt{(1/F)}$. The representation used by Hafner[3] is in terms of v_a/U_T and v_i/U_T, where $v_a/U_T = \sqrt{(1/f_a)}$ and $v_i/U_T = \sqrt{(1/f_i)}$. These relationships are termed ' characteristic curves.'

The sign convention adopted is that the thrust is essentially positive, and v_a and v_i are positive when in opposite sense to the thrust.

6.2. *Reduction of Experimental Results.—The rotor blade pitch angle* vs. *rate of descent curve.*

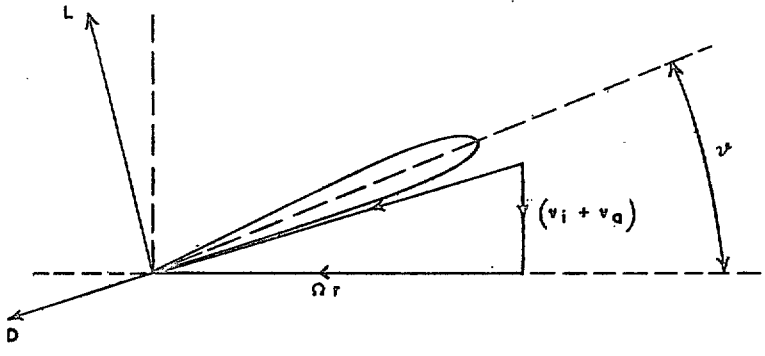

From the geometry of the diagram representing conditions of flow at an elemental radius of the rotor blade we have:—

$$dT \simeq \frac{\rho}{2}\left(\vartheta - \frac{v_i + v_a}{\Omega r}\right)\frac{dC_L}{d\alpha} Cb\Omega^2 r^2\, dr \quad .. \quad .. \quad .. \quad .. \quad .. \quad .. \quad (1)$$

where

ϑ is the blade angle measured from the angle of zero lift

r the elemental radius

C the chord at the elemental radius

b the number of blades (3)

Ω the angular velocity, radn/sec (23·5)

$dC_L/d\alpha$ the two-dimensional lift slope, C_L/radn (5·6).

Integration of this equation using the actual blade plan form gives an expression for the total thrust. This, when equated to the weight of the helicopter (2750 lb), gives the following expression for the mean induced velocity in terms of the blade angle, and the axial velocity at infinity (rate of descent):—

$$v_i = 284{\cdot}5\vartheta - v_a - 26{\cdot}3.$$

It should be remembered that the value of the mean induced velocity calculated from this formula is fictitious in the vortex ring and part of the windmill brake states of operation of the rotor, and is only of use in conjunction with the experimentally determined rate of descent corresponding to the same pitch angle.

Using the curve of Fig. 3, the expression for the induced velocity v_i, and the definitions given in section 6.1 the curves of v_a/U_T against U/U_T and v_a/U_T against v_i/U_T are given in Figs. 5 and 6 respectively.

The rotor power vs. *rate of descent curve.*

From the diagram of conditions at a blade element we have:—

$$dP \simeq \left[\left(\vartheta - \frac{v_i + v_a}{\Omega r}\right)\left(v_i + v_a\right)\frac{dC_L}{d\alpha} + C_{D0}\Omega r\right] bC\frac{\rho}{2}\Omega^2 r^2\, dr \qquad \ldots \quad \ldots \quad \ldots \quad (2)$$

where

dP is the increment in power required at the element dr and C_{D0} is the section profile drag coefficient.

With v_i assumed constant over the rotor disc, integration of equation (2) gives for the helicopter in vertical descent—

$$P = W(v_i + v_a) + P_p \qquad \ldots \quad \ldots \quad \ldots \quad \ldots \quad \ldots \quad \ldots \quad (3)$$

where

P is the power supplied to the rotor

and P_p is the rotor profile power.

It should be remembered that in reality the induced velocity v_i is a function of the radius. The tests established the numerical integral values of equations (1) and (2) taking into account the actual distribution of induced velocity. Therefore the mean v_i defined by equation (1) will differ from that given by equation (2). This difference will depend on how far the supposition of a constant induced velocity is from the truth. Calculation shows that for an induced velocity increasing linearly with the radius to the tip the difference in hovering flight, the worst case, is only 3 per cent.

Using the rotor power—rate of descent relationship of Fig. 4 and equation (3) curves of v_a/U_T against U/U_T and v_a/U_T against v_i/U_T were calculated, and are shown in Figs. 5 and 6 respectively. The value of the profile drag power, 46·2 h.p., was obtained by correcting the value given in R. & M. 2521[5] for the difference in main rotor speed.

7. *Analysis of Smoke Patterns.*—Typical photographs obtained from the tail camera illustrating the types of flow associated with various rates of descent are given in Figs. 9 and 10.

The blades are advancing towards the camera lens. When a blade lies in the plane contained by the boom and the rotor shaft, the tip appears directly over a point just inboard of the outer end of the boom. When the tip appears to the left or right of this point the blade is in a position before or after the plane contained by the boom and rotor shaft which is also the plane of the smoke unless otherwise stated.

Fig. 9 (1) shows the type of flow at a rate of descent of 400 ft/min. The two inner smoke streamers are directed downwards indicating a flow through the rotor continuing well below the rotor disc. Eventually the down-going air is deflected radially outwards, and upwards by the up-coming air, this process being accompanied by turbulent mixing of the two opposing air streams. Air consisting of part of the old slipstream and that entrained by mixing is then drawn in over the rotor. This passing of individual particles of air more than once through the rotor characterises the vortex ring state of operation.

Fig. 9 (2) shows the type of flow at a rate of descent of 600 ft/min using a single smoke filament at 0·7 of the rotor radius. This photograph illustrates the vortex ring state of operation very clearly. Due to a slight backward velocity of the rotor, however, the section of the 'vortex ring' depicted is not strictly in the plane contained by the boom and the rotor shaft, but is a helix cutting the rotor disc at different positions.

Fig. 9 (3) illustrates the type of flow at a rate of descent of 1400 ft/min. The air is still flowing downwards through the rotor, but the centre of the vortex is now well above the rotor. The vortex circulation appears to be smaller than that in the previous paragraph. The up-coming air progresses undeflected nearer to the plane of the rotor disc at the inner radii than the outer. This indicates a larger downward flow near the blade tip than near the root.

Fig. 10 (4) shows the conditions of flow at 1700 ft/min. There appears to be a small upward flow through the disc at the inner radii, but a small downward flow towards the tip and the resultant vortex system lying mainly above the blade still exists at the outer radii.

Fig. 10 (5) shows the flow at a rate of descent of 2000 ft/min where there is an established upward flow at the inner radii of the disc, but at the tip it is very difficult to see if any small downward flow still remains, or if a condition of zero flow exists. It is clear that this photograph illustrates conditions pertaining to the end of the vortex ring state of operation, that is when the mean value of the flow through the rotor is zero. This state is called ideal autorotation. The rotor would not actually autorotate in this condition because an upward flow through the rotor is necessary to overcome the profile drag of the blades, transmission friction torque, and the tail rotor torque. A study of Fig. 4 shows that the rate of descent at which the engine is supplying the torque necessary to balance these losses is just over 2250 ft/min. This is the rate of descent when the engine power supplied to the main rotor itself is 46·2 h.p.—the value of the profile drag power. The agreement therefore between the rate of descent from power considerations *i.e.* 2250 ft/min, and that indicated by the smoke pattern, approximately 2000 ft/min is very good.

Fig. 10 (6) shows the conditions of flow at a rate of descent of 2400 ft/min with the smallest pitch angle obtainable on the *Hoverfly I*. It will be seen that the flow is upwards over the whole of the rotor disc which is now operating in the windmill brake state, characterised by the upward flow through the rotor. Energy from the air flowing through the disc is being used in overcoming the losses mentioned in the previous paragraph.

A series of diagrams has been constructed from various photographs obtained for each state and are given with associated photographs in Figs. 9 and 10. These diagrams give a general physical picture of the flow conditions for a helicopter rotor for the range from just below hovering down to complete autorotation.

8. *Discussion.*—In Figs. 7 and 8, the two characteristic curves obtained in flight are compared with those obtained by wind-tunnel tests (R. & M. 1014[1]) on model propellers of fine pitch. Also plotted are curves obtained by the simple vortex theory where applicable.

When comparing the two curves obtained from flight with those from wind-tunnel tests the following points should be borne in mind.

When a rotor or propeller is operating in the vortex ring state, viscous forces play a large part in determining the flow pattern. The characteristic curves may therefore be subject to scale effect.

The curves obtained from wind-tunnel tests may be in error due to the uncertain nature of the wind-tunnel constraint in the vortex ring state of operation. The vertical drag of the fuselage has not been taken into account in producing the flight curves, due to the uncertain nature of the flow. The error introduced is likely to be small.

With regard to the discrepancy between the two flight curves, this may be due to experimental error. The engine powers as obtained from the maker's charts are subject to an error of $\pm$ 2·5 per cent and the estimation of tail rotor power, transmission loss, and engine cooling fan power are other sources of error. Also the twisting and distortion of the rotor blades are unknown quantities. However considering the intrinsic difficulties of accurate measurements in the vortex ring state of operation the agreement is very good.

9. *Conclusions.*—The smoke photographs give a good physical picture of the various types of flow associated with the vertical descent of a helicopter as it passes from near hovering through the vortex ring and into the windmill brake states of operation.

The rate of descent at which ideal autorotation occurs as obtained from the smoke photographs is in good agreement with that obtained from power considerations.

The mean of the two characteristic curves obtained in flight represents fairly accurately conditions pertaining to the *Hoverfly I*, and could be used with confidence to estimate the performance in vertical descent of other helicopters with single rotors of roughly similar dimensions.

REFERENCES

No.	*Author*	*Title, etc.*
1	C. N. H. Lock and others	An Extension of the Vortex Theory of Airscrews with Applications to Airscrews of Small Pitch, including Experimental Results. R. & M. 1014.
2	G. S. Hislop	Comparison Between the Measured Performance of a *Hoverfly I* Aircraft in Vertical Flights and the Characteristic Curve of an Airscrew. Technical Note No. Aero. 1837. A.R.C. No. 19210. (Unpublished.)
3	R. Hafner	Rotor Systems and Control Problems in the Helicopter. (Anglo-American Aeronautical Conference) Sept. 1947.
4	W. Stewart	General Handling Tests of the *Sikorsky R-4B* Helicopter (*Hoverfly I*). R. & M. 2431. October, 1946.
5	P. Brotherhood	An Investigation in Flight of the Induced Velocity Distribution under a Helicopter Rotor when Hovering. Report No. Aero. 2212. R. & M. 2521. June, 1947.
6	C. N. H. Lock	Note on the Characteristic Curve for an Airscrew or Helicopter. R. & M. 2673. June, 1947.

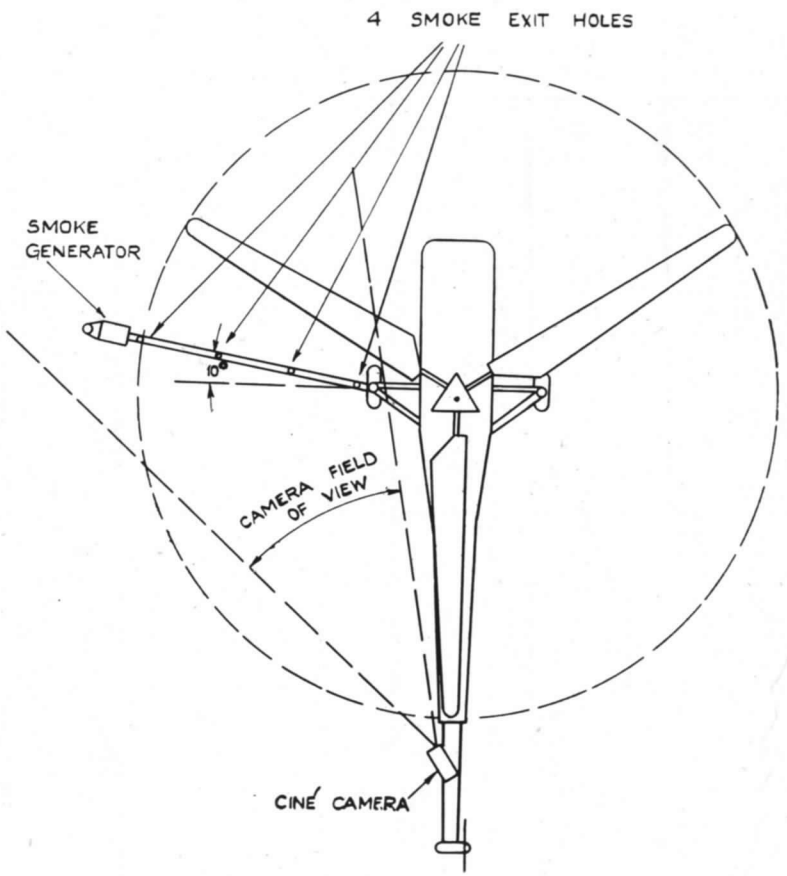

FIG. 1. Diagrammatic layout of smoke installation.

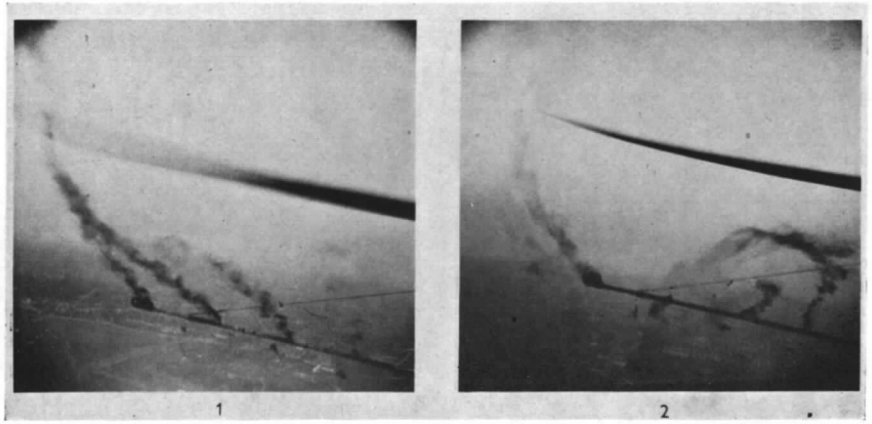

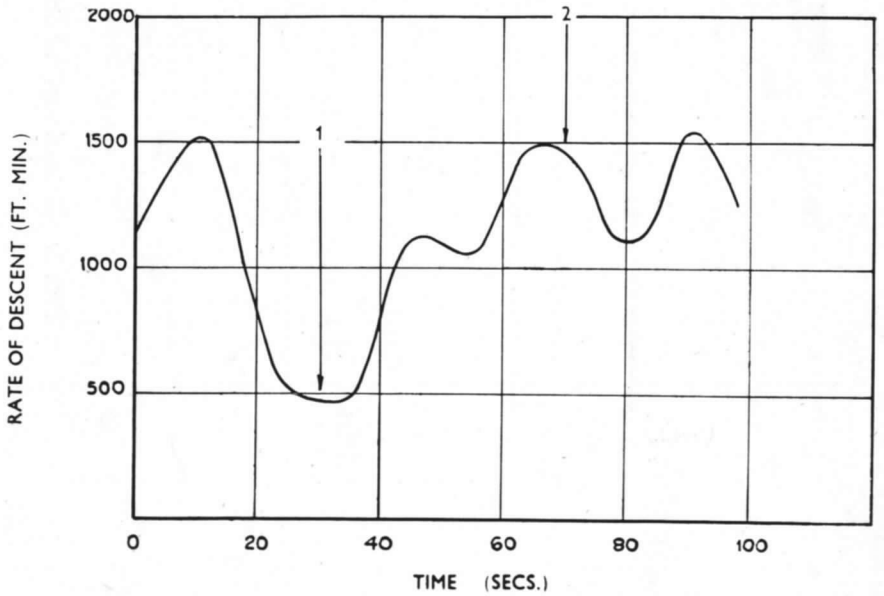

FIG. 2. A typical time history of a vertical descent.

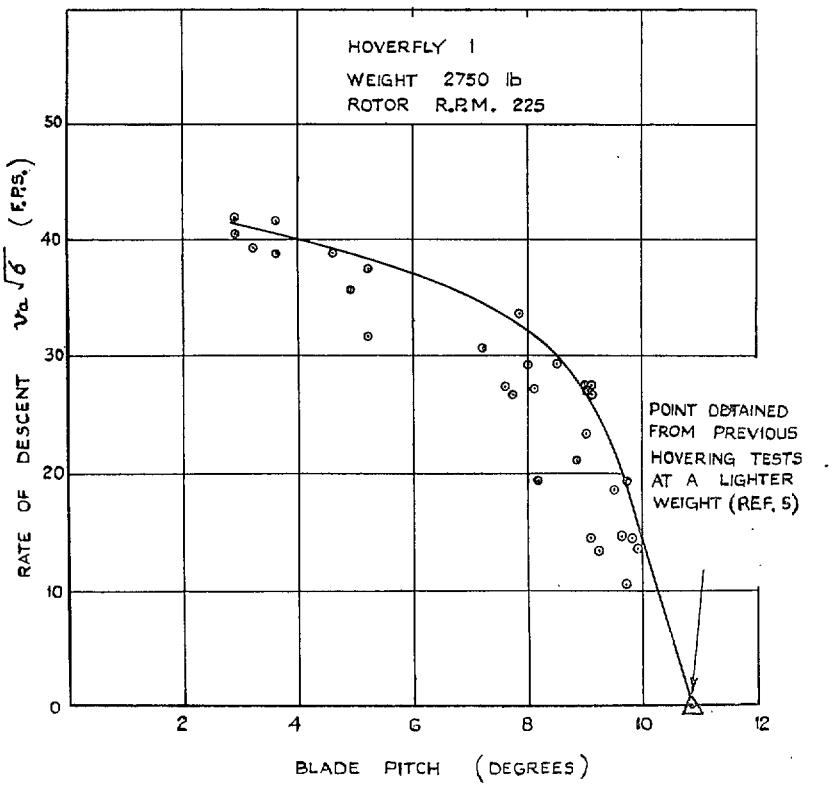

FIG. 3. Rate of vertical descent *vs.* blade pitch.

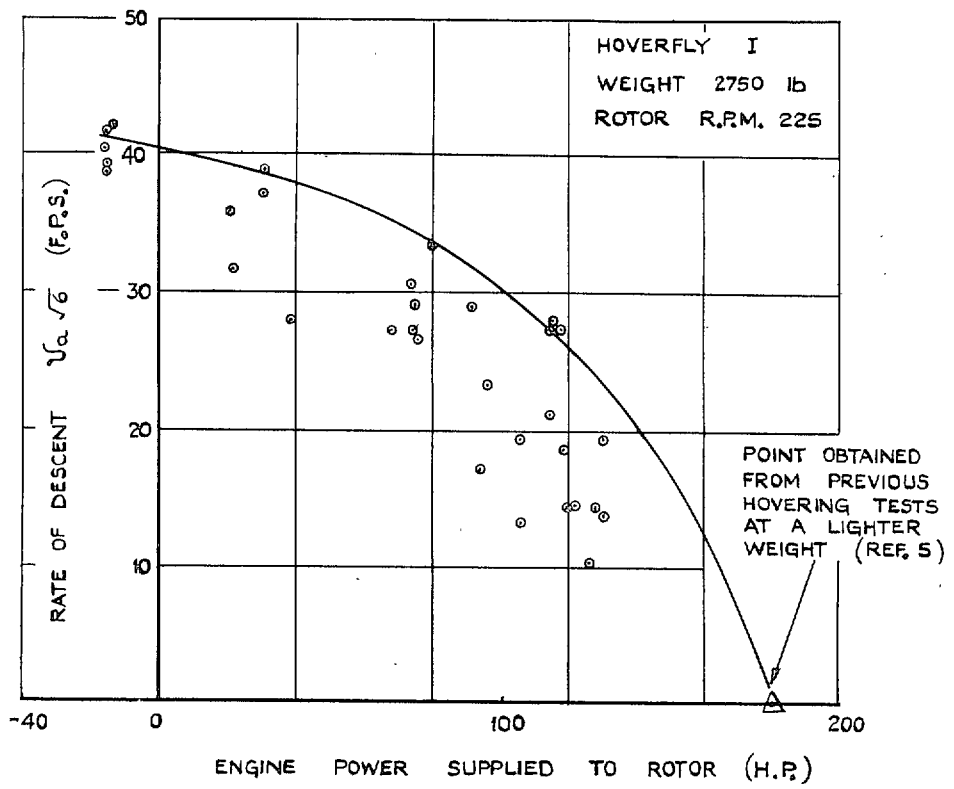

FIG. 4. Rate of vertical descent *vs.* engine power supplied to rotor.

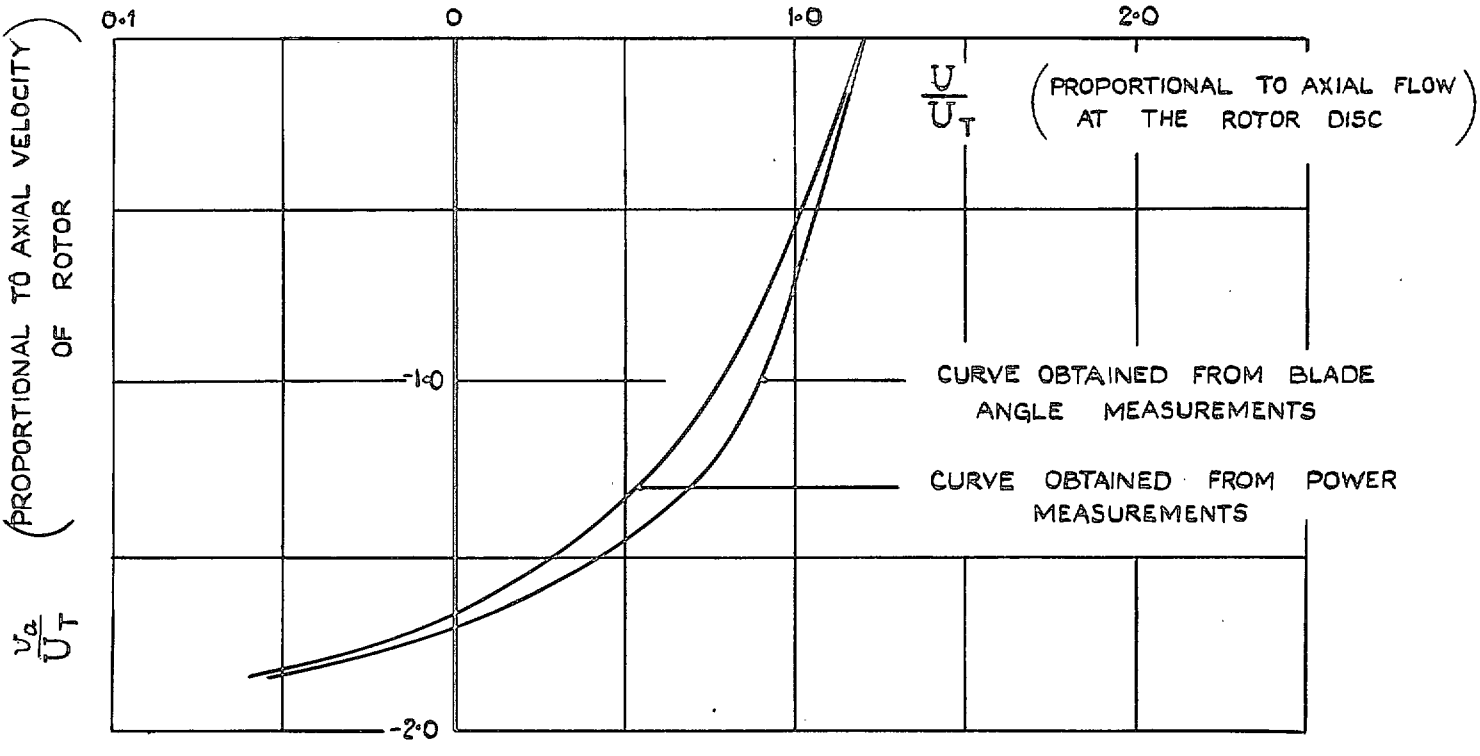

FIG. 5. Characteristic curves obtained from flight measurements (Lock's presentation).

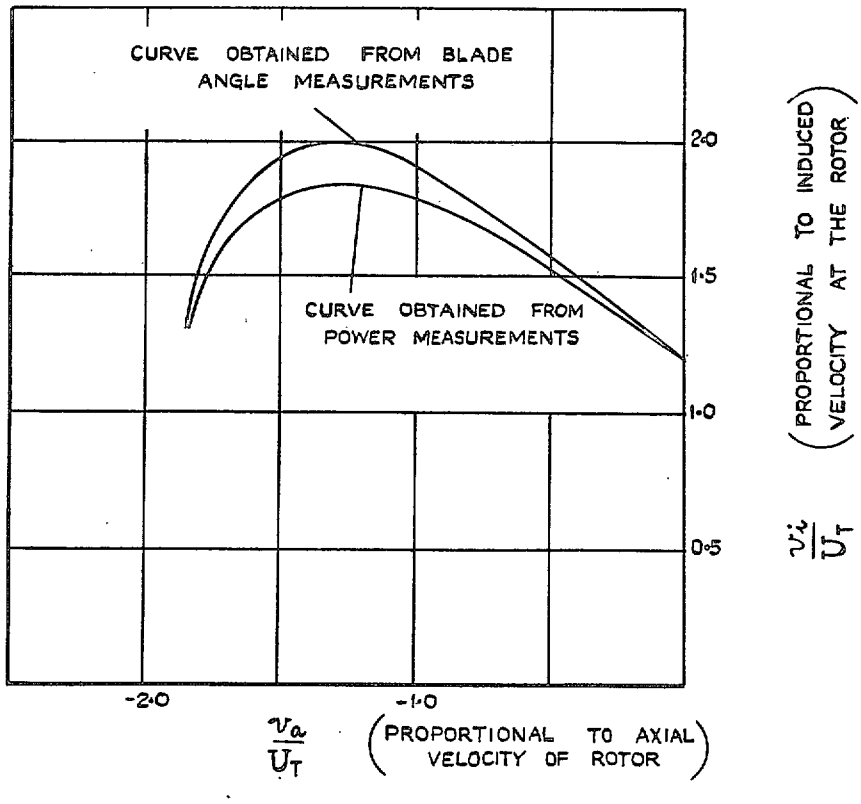

FIG. 6. Characteristic curves obtained from flight measurements (Hafner's presentation).

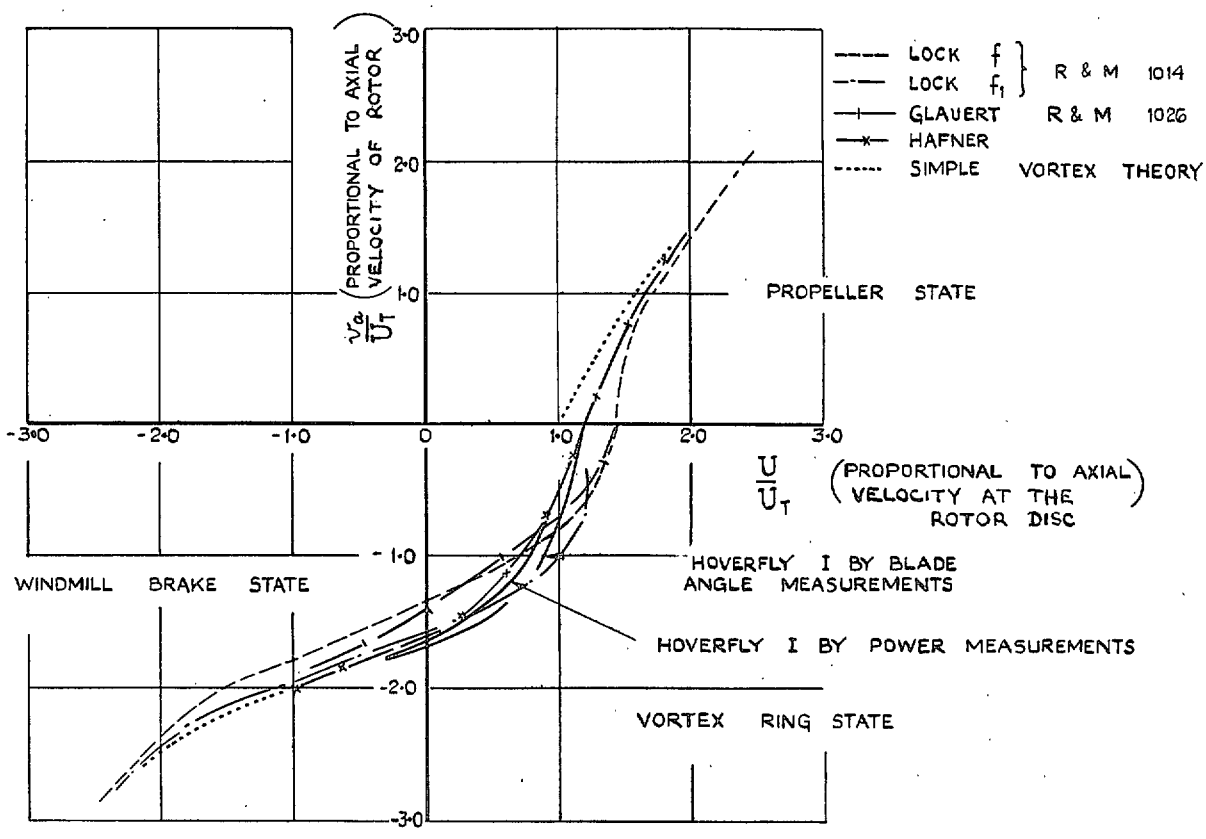

FIG. 7. A comparison of the characteristic curves obtained from flight measurements and those obtained from wind-tunnel tests on fine pitch propellers (Lock's presentation).

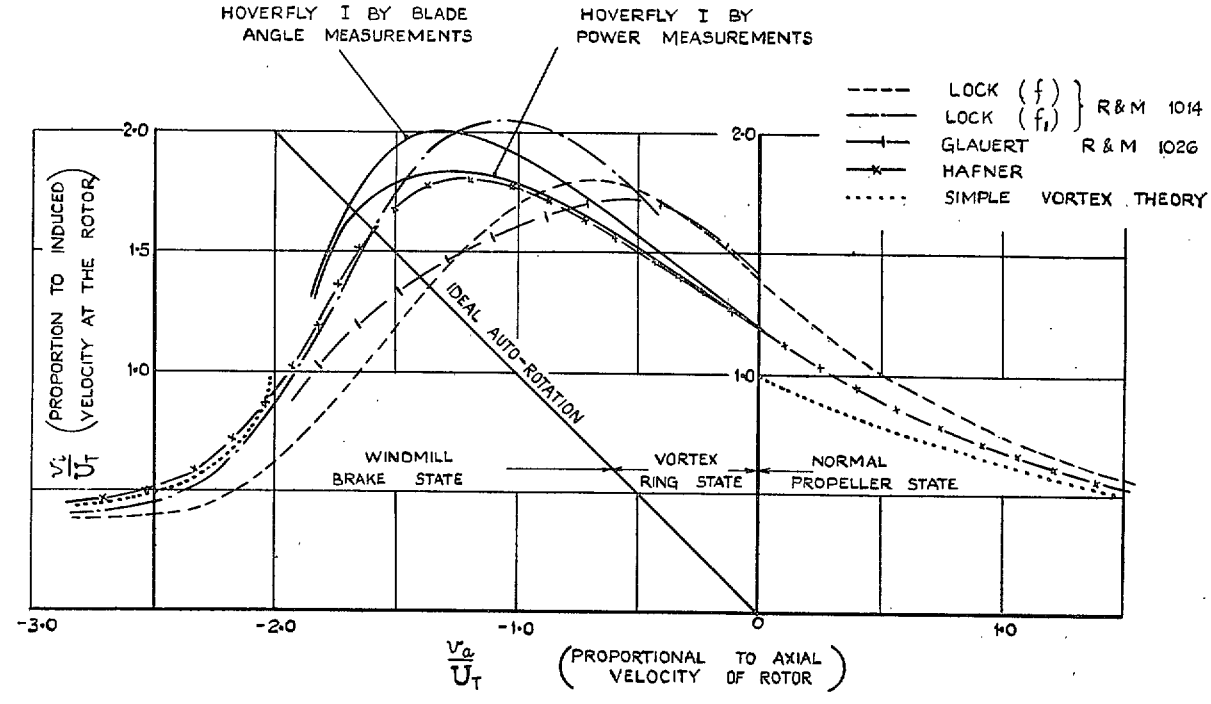

FIG. 8. A comparison of the characteristic curves obtained from flight measurements and those obtained from wind-tunnel tests on fine pitch propellers (Hafner's presentation).

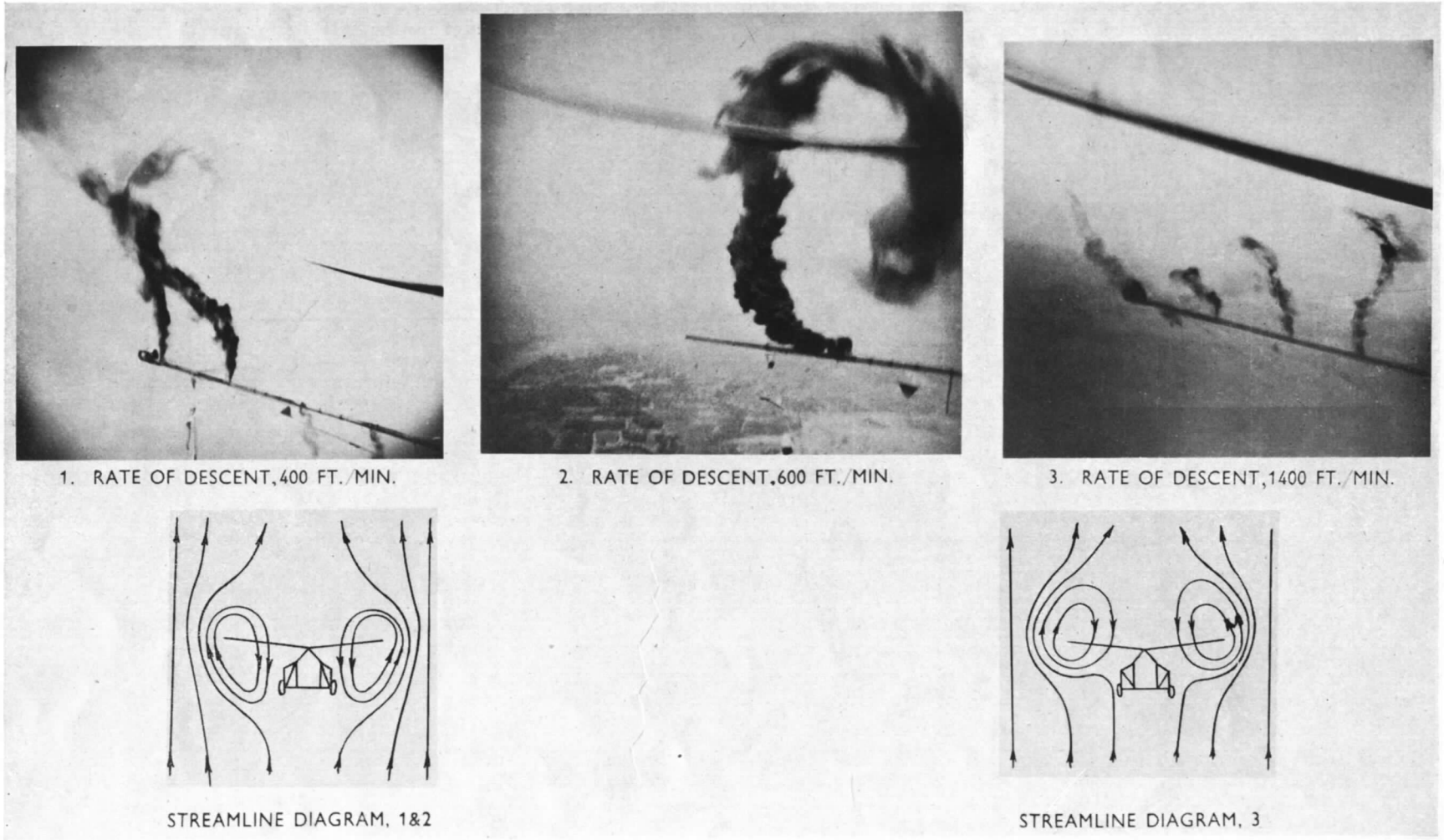

FIG. 9. Photographs and diagrams illustrating types of flow during vertical descent.

(22735) Wt. 15-680 K9 6/52 F. M. & S.

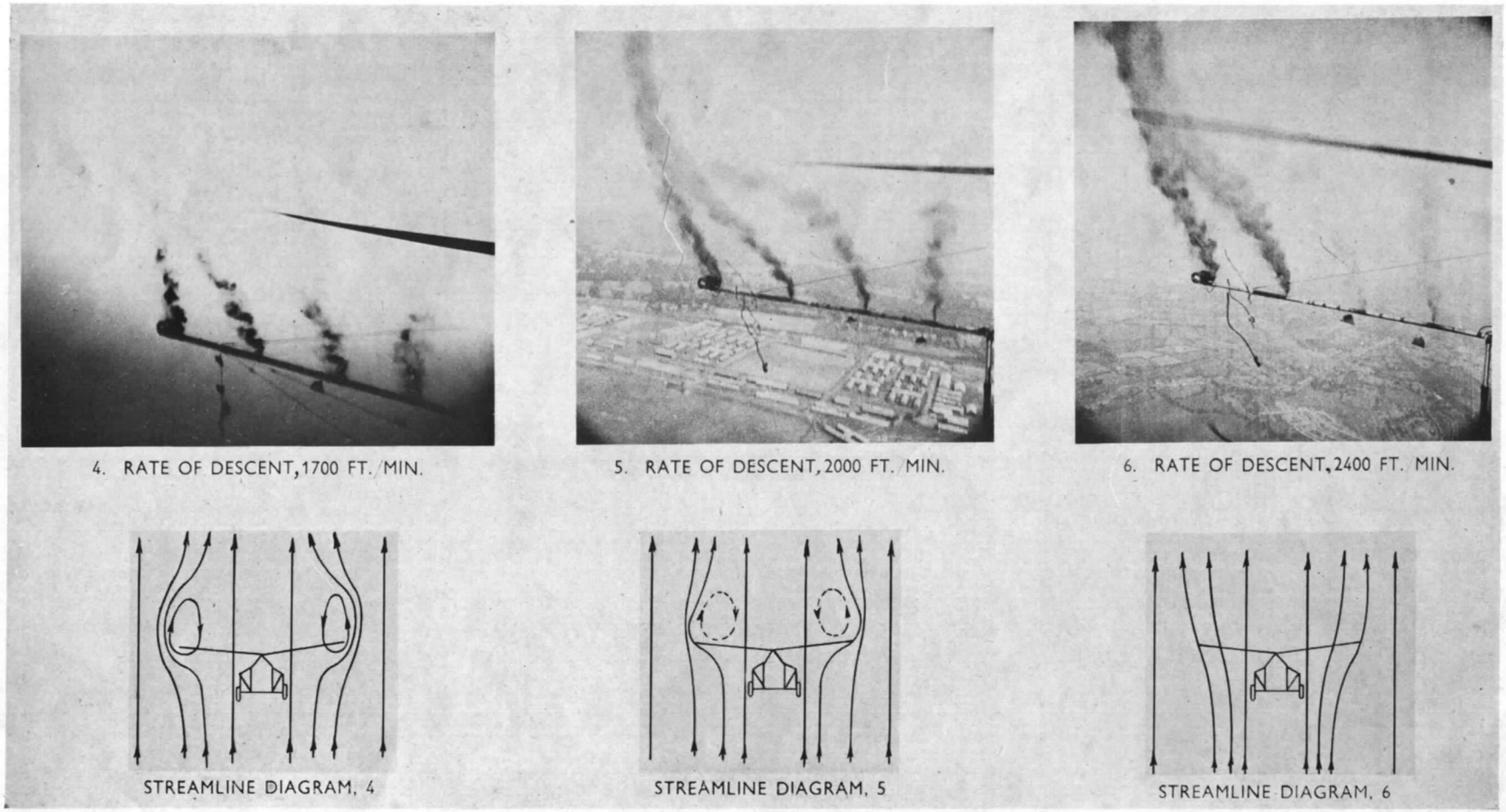

FIG. 10. Photographs and diagrams illustrating types of flow during vertical descent.

PRINTED IN GREAT BRITAIN

Publications of the Aeronautical Research Council

ANNUAL TECHNICAL REPORTS OF THE AERONAUTICAL RESEARCH COUNCIL (BOUND VOLUMES)—

1934–35 Vol. I. Aerodynamics. *Out of print.*
Vol. II. Seaplanes, Structures, Engines, Materials, etc. 40*s.* (40*s.* 8*d.*)

1935–36 Vol. I. Aerodynamics. 30*s.* (30*s.* 7*d.*)
Vol. II. Structures, Flutter, Engines, Seaplanes, etc. 30*s.* (30*s.* 7*d.*)

1936 Vol. I. Aerodynamics General, Performance, Airscrews, Flutter and Spinning. 40*s.* (40*s.* 9*d.*)
Vol. II. Stability and Control, Structures, Seaplanes, Engines, etc. 50*s.* (50*s.* 10*d.*)

1937 Vol. I. Aerodynamics General, Performance, Airscrews, Flutter and Spinning. 40*s.* (40*s.* 10*d.*)
Vol. II. Stability and Control, Structures, Seaplanes, Engines, etc. 60*s.* (61*s.*)

1938 Vol. I. Aerodynamics General, Performance, Airscrews. 50*s.* (51*s.*)
Vol. II. Stability and Control, Flutter, Structures, Seaplanes, Wind Tunnels, Materials. 30*s.* (30*s.* 9*d.*)

1939 Vol. I. Aerodynamics General, Performance, Airscrews, Engines. 50*s.* (50*s.* 11*d.*)
Vol. II. Stability and Control, Flutter and Vibration, Instruments, Structures, Seaplanes, etc. 63*s.* (64*s.* 2*d.*)

1940 Aero and Hydrodynamics, Aerofoils, Airscrews, Engines, Flutter, Icing, Stability and Control, Structures, and a miscellaneous section. 50*s.* (51*s.*)

Certain other reports proper to the 1940 *volume will subsequently be included in a separate volume.*

ANNUAL REPORTS OF THE AERONAUTICAL RESEARCH COUNCIL—

1933–34 1*s.* 6*d.* (1*s.* 8*d.*)
1934–35 1*s.* 6*d.* (1*s.* 8*d.*)
April 1, 1935 to December 31, 1936. 4*s.* (4*s.* 4*d.*)
1937 2*s.* (2*s.* 2*d.*)
1938 1*s.* 6*d.* (1*s.* 8*d.*)
1939–48 3*s.* (3*s.* 2*d.*)

INDEX TO ALL REPORTS AND MEMORANDA PUBLISHED IN THE ANNUAL TECHNICAL REPORTS, AND SEPARATELY—

April, 1950 R. & M. No. 2600. 2*s.* 6*d.* (2*s.* 7½*d.*)

INDEXES TO THE TECHNICAL REPORTS OF THE AERONAUTICAL RESEARCH COUNCIL—

December 1, 1936 — June 30, 1939. R. & M. No. 1850. 1*s.* 3*d.* (1*s.* 4½d.)
July 1, 1939 — June 30, 1945. R. & M. No. 1950. 1*s.* (1*s.* 1½*d.*)
July 1, 1945 — June 30, 1946. R. & M. No. 2050. 1*s.* (1*s.* 1½*d.*)
July 1, 1946 — December 31, 1946. R. & M. No. 2150. 1*s.* 3*d.* (1*s.* 4½*d.*)
January 1, 1947 — June 30, 1947. R. & M. No. 2250. 1*s.* 3*d.* (1*s.* 4½*d.*)

Prices in brackets include postage.

Obtainable from

HER MAJESTY'S STATIONERY OFFICE

York House, Kingsway, LONDON, W.C.2 423 Oxford Street, LONDON, W.1
P.O. Box 569, LONDON, S.E.1
13a Castle Street, EDINBURGH, 2 1 St. Andrew's Crescent, CARDIFF
39 King Street, MANCHESTER, 2 Tower Lane, BRISTOL, 1
2 Edmund Street, BIRMINGHAM, 3 80 Chichester Street, BELFAST

or through any bookseller.